Quasi-static analysis of controllable optical cross-sections of a layered nanoparticle with a sandwiched gain layer

2014 J. Opt. 16 075003

(http://iopscience.iop.org/2040-8986/16/7/075003)

IOP Publishing Journal of Optics
J. Opt. **16** (2014) 075003 (6pp) doi:10.1088/2040-8978/16/7/075003

Quasi-static analysis of controllable optical cross-sections of a layered nanoparticle with a sandwiched gain layer

Weiren Zhu[1], Malin Premaratne[1], Sarath D Gunapala[2], Govind P Agrawal[3] and Mark I Stockman[4]

[1] Advanced Computing and Simulation Laboratory (A χ L), Department of Electrical and Computer Systems Engineering, Monash University, Victoria 3800, Australia
[2] Jet Propulsion Laboratory, California Institute of Technology, Pasadena, CA 91109, USA
[3] The Institute of Optics, University of Rochester, Rochester, NY 14627, USA
[4] Department of Physics and Astronomy, Georgia State University, Atlanta, GA 30303, USA

E-mail: weiren.zhu@monash.edu

Received 27 March 2014, revised 27 May 2014
Accepted for publication 3 June 2014
Published 25 June 2014

Abstract

We theoretically study the optical performance of a layered nanoparticle with a sandwiched gain shell. Based on quasi-static analysis and full-wave numerical simulations, we show that it is possible to achieve a very high scattering cross-section (over 4 orders) accompanied with a negative absorption cross-section by changing the amount of gain in the sandwiched shell layer. This suggests that the proposed configuration can either be used for designing a spaser or as a switchable nano scatterer whose scattering cross-section can be manipulated from an ultra-high value to an ultra-low one. To provide more insight into the operation of this proposed configuration, we also study the near field, which again confirms a clear controllability of field enhancement through the sandwiched gain layer.

Keywords: nanoshell, gain, spaser

(Some figures may appear in colour only in the online journal)

1. Introduction

During the last decade or so, considerable interest has been focused on the surface plasmon amplification by stimulated emission of radiation, named spaser or plasmon laser [1–5]. A spaser can be made by a plasmonic nanoparticle (or by an array of such nanoparticles) containing a gain medium, resulting in a configuration similar to a resonant cavity of a laser [6–9]. The energy of the gain medium in the spaser can be transferred to the metallic component to completely compensate the ohmic losses and thus results in an extreme amplification of surface plasmon resonance [1, 10]. Different from semiconductor based lasers whose sizes remain on the scale of micrometer or millimeter owing to the well-known diffraction limit of optics, the physical size of a spaser can be deeply subwavelength, i.e., on the scale of several nanometers. This opens up a wide range of applications of spasers, including nanoscale lithography, biosensing, microscopy, data storage, and on-chip surface plasmon generation [10, 11].

Since Bergman and Stockman [1] theoretically proposed the concept of spaser, various theoretical schemes and experimental demonstrations have been carried out on the amplification of localized or propagating surface plasmons using plasmonic configurations such as nanospheres [12], nanorods [13], split-ring resonators [6], or metallic channel [14]. Among various plasmonic nanoparticles, metallic nanospheres or nanoshells are of particular interest owing to their relatively simpler geometry and polarization insensitive plasmonic properties [15, 16], and gain-assisted nanosphere and nanoshell have been well demonstrated for surface plasmon amplification [5, 12, 17].

Compared with nanospheres and nanoshells, metal–dielectric–metal core/shell/shell nanoparticles show more flexible tunebility and more colorful plasmonic features, that have been well studied in literature [18–20]. However, no spaser

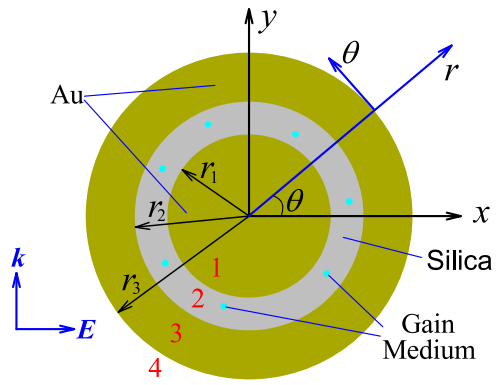

Figure 1. Schematic of a gain-assisted metal–dielectric–metal layered nanosphere configuration. Gain medium doped in the sandwiched dielectric layer.

has been reported based on this composite configuration. In this paper, we theoretically propose a gain-assisted core/shell/shell nanoparticle which can be used for designing a spaser. The surface plasmon amplification features of this nanoparticle are investigated by quasi-static analysis and finite-element simulation. We demonstrate that a strongly amplified scattering cross-section accompanied with a negative absorption cross-section can be realized by introducing a suitable amount of gain into the proposed nanoparticle. However, without loss of generality, we do not identify a specific gain mechanism for the gain medium. It could be either optically pumped [21] or electrically injected [22]. The near field of the proposed configuration is further studied, which shows a clear controllability of field enhancement through modulating the optical gain in the dielectric medium.

2. Analysis and discussion

In figure 1, we show the proposed configuration composed of metal–dielectric–metal layered concentric sphere structure with a shell-shaped gain medium sandwiched by a metallic core and an outer shell. It is assumed that the whole nano particle is suspended in free space. The radii of the metal core, dielectric shell, and metal shell are denoted as r_1, r_2, and r_3, respectively. The dielectric shell is assumed to be made of silica and the effective permittivity of the gain layer is characterized as $\varepsilon_d = 2.04 - i\varepsilon''$, where the imaginary part represents the level of optical gain. The metallic parts are gold with effective Drude-model permittivity $\varepsilon_m = \varepsilon_\infty - \omega_p^2/\left(\omega^2 + i\omega\gamma\right)$, where $\omega = 2\pi f$ is the angular frequency, $\varepsilon_\infty = 9.5$, and $\omega_p = 1.36 \times 10^{16}$ rad s^{-1} is the plasmonic frequency [23, 24]. Since in our case the sizes of the gold core and shell are less than the mean free path of electrons, the electron surface scattering should be considered. For simplicity, we choose $\gamma = 1.92 \times 10^{14}$ rad s^{-1} which is twice of the bulk gold's collision frequency.

Assuming that the size of the proposed nanoparticle is much smaller than the operating wavelength, quasi-static theory and electrostatic potential can be employed for the characterization of its electromagnetic performance. Under this assumption, the electrostatic potential $\Phi_i(r, \theta, \phi)$ in each layer of the nanoparticle can be obtained by solving the Laplace equation $\nabla^2\Phi_i = 0$ in the spherical coordinate, from which we are able to determine the electric field, $\vec{E}_i = -\nabla\Phi_i$. Here, the subscript i = 1, 2, 3, or 4 denotes each layer as shown in figure 1. Due to the azimuthal symmetry of the system, Φ_i is independent on ϕ, and its general solution is of the form [25]

$$\Phi_i(r, \theta) = \sum_{n=0}^{\infty}\left[A_{i,n}r^n + B_{i,n}/r^{n+1}\right]P_n(\cos\theta), \tag{1}$$

where $P_n(\cos\theta)$ is the Legendre Polynomial of order n, θ is the polar angle, and coefficients $A_{i,n}$ and $B_{i,n}$ are constants. When an x-polarized light with amplitude E_0 incident from the y direction, $B_{1,n}$ must vanish in order to keep the electric field finite at the centre of sphere. On another hand, the electric field amplitude in a position far away from the nanoparticle ($r \to \infty$) trends to the incident value E_0, such that we get $A_{4,n} = -E_0\delta_{n,1}$ with δ being Kronecker's delta.

The continuity of the the electric field's tangential component and the equality of the displacement field's normal component at each interface ($r = r_i$) demand

$$\partial\Phi_i/\partial\theta = \partial\Phi_{i+1}/\partial\theta, \tag{2a}$$

$$\varepsilon_i\partial\Phi_i/\partial r = \varepsilon_{i+1}\partial\Phi_i/\partial r, \tag{2b}$$

where ε_i is the relative permittivity of the medium occupies in the i-th layer, i.e., $\varepsilon_1 = \varepsilon_3 = \varepsilon_m$, $\varepsilon_2 = \varepsilon_d$, and $\varepsilon_4 = 1$. With the boundary conditions as described in equation (2), the parameters in equation (1) can be solved in each layer,

$$A_{1,n} = \frac{27\varepsilon_m\varepsilon_d r_2^3 r_3^3}{\xi}E_0\delta_{n,1}, \tag{3a}$$

$$A_{2,n} = \frac{\varepsilon_m + 2\varepsilon_d}{3\varepsilon_d}A_{1,n}, \tag{3b}$$

$$B_{2,n} = \frac{(\varepsilon_d - \varepsilon_m)r_1^3}{3\varepsilon_d}A_{1,n}, \tag{3c}$$

$$A_{3,n} = \frac{2\varepsilon_m + \varepsilon_d}{3\varepsilon_m}A_{2,n} - \frac{2(\varepsilon_m - \varepsilon_d)^2 r_1^3}{9\varepsilon_m\varepsilon_d r_2^3}A_{1,n}, \tag{3d}$$

$$B_{3,n} = \frac{(\varepsilon_m + 2)r_3^3 A_{3,n} + 3r_3^3 E_0\delta_{n,1}}{2(\varepsilon_m - 1)}, \tag{3e}$$

$$B_{4,n} = \left(A_{3,n} + E_0\right)r_3^3 + B_{3,n}, \tag{3f}$$

where

$$\xi = \left(2r_2^6 - 2r_1^3 r_2^3\right)(\varepsilon_m + 2\varepsilon_d)(\varepsilon_d - \varepsilon_m)(1 - \varepsilon_m) + \eta(\varepsilon_m + 2),$$

and

$$\eta = 2r_1^3 r_3^3(\varepsilon_d - \varepsilon_m)^2 - r_2^3 r_3^3\left(2\varepsilon_m^2 + 5\varepsilon_m\varepsilon_d + 2\varepsilon_d^2\right).$$

The electrostatic potential in the region outside the nanoparticle can be physically interpreted as the superposition of the external field $\vec{E}_0$ and the scattering of an effective

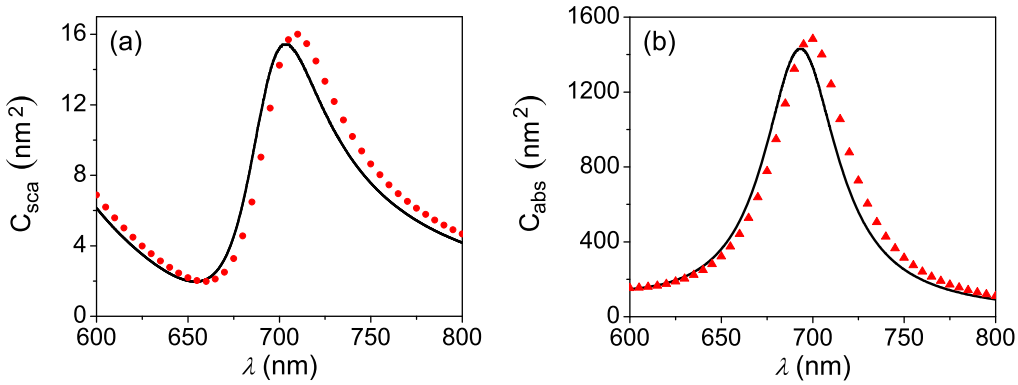

Figure 2. (a) Scattering cross-section and (b) absorption cross-section of the core/shell/shell nanoparticle without gain. Solid curves and discrete dots refer to the results by quasi-static analysis and numerical simulations, respectively.

dipole $\vec{p} = \alpha\vec{E}_0$ located at the center of the nanoparticle,

$$\Phi_4 = -\vec{E}_0 \cdot \vec{r} + \frac{\vec{p} \cdot \vec{r}}{4\pi\varepsilon_0 r^3}, \tag{4}$$

with the polarizability α given by

$$\alpha = \frac{2\pi r_3^3}{\varepsilon_m - 1}\left(2\varepsilon_m + 1 - 9\varepsilon_m \eta/\xi\right). \tag{5}$$

Once the polarizability is known, the scattering and absorption cross-sections can be obtained by the relations [25]

$$C_{sca} = k_0^4 |\alpha|^2/(6\pi), \tag{6a}$$

$$C_{abs} = k_0 \,\mathrm{Im}\,(\alpha), \tag{6b}$$

where k_0 is the wavevector in free space. We will show the optical cross-sections of the proposed nanoparticle changes significantly when sandwiched gain layer strength is varied.

To illustrate this point, we consider the following model configuration. Consider a core/shell/shell nanoparticle with radii $r_1 = 10$ nm, $r_2 = 14$ nm, and $r_3 = 20$ nm. In figure 2 we first show the scattering and absorption cross-sections calculated by equation (6) in the case where gain is switched off ($\varepsilon'' = 0$). We see that the scattering curve shows a peak at 704 nm and a dip at 654 nm. The quality factor, estimated by the resonant wavelength over the spectral linewidth, $Q = \lambda_{res}/\Delta\lambda$, is as low as 11 for the scattering peak. Meanwhile, the absorption curve shows a peak around 697 nm. It is seen that the peak value of the scattering cross-section (15.4 nm^2) is significantly smaller than that of the absorption cross-section (1431 nm^2), simply because C_{sca} ($\propto r_3^6$) scales much faster than C_{abs} ($\propto r_3^3$) as the size of the nanoparticle reduces.

The accuracy of the above quasi-static analysis is examined by numerical simulations based on a finite elements method. The scattering and absorption cross-sections can be numerically calculated from the Poynting theorem [5],

$$C_{sca} = \frac{1}{2I_{inc}}\,\mathrm{Re}\left\{\int\!\!\int_S \left(\vec{E}_s \times \vec{H}_s^*\right)\cdot \hat{n}\mathrm{d}S\right\}, \tag{7a}$$

$$C_{sca} = -\frac{1}{2I_{inc}}\,\mathrm{Re}\left\{\int\!\!\int_S \left(\vec{E}_{tot} \times \vec{H}_{tot}^*\right)\cdot \hat{n}\mathrm{d}S\right\}, \tag{7b}$$

where S is a spherical surface surrounding the nanoparticle in the far field, I_{inc} is the incident irradiance $\vec{E}_s$ and $\vec{H}_s$ are the scattered electric and magnetic fields, and $\vec{E}_{tot}$ and $\vec{H}_{tot}$ refer to the total electric and magnetic fields. The simulated scattering and absorption cross-sections are also plotted in figure 2. We see that these results are in excellent agreement with those of quasi-static analysis, except for the slight red-shifts in both curves, where the scattering peak moves towards 710 nm and the absorption peak shifts towards 700 nm. This verifies the high accuracy of our quasi-static analysis for the proposed nanoparticle model. It is worth noting that the accuracy of the theoretical model is highly dependent on the nanoparticle size. When the nanoparticle is significantly small (e.g., less than 5 nm), quantum size effects do play a significant role and must be accounted for. On the other extreme scenario where the nanoparticle is significantly large (e.g., more than 50 nm), quasi-static approximation becomes less accurate because the field is not uniform everywhere in the particle.

Figure 3 shows the scattering cross-section of the proposed nanoparticle as a function of optical gain (ε'') and wavelength (λ) using equation (6). Similar to a metallic nanosphere or a nanoshell based spaser, the C_{sca} peak in our work increases rapidly when gain medium is introduced into the dielectric layer and reaches its maximal value of 2.88×10^5 nm^2 at $\lambda = 695$ nm and $\varepsilon'' = 0.265$. This value is over 10^4 times larger than the peak C_{sca} value of the nano particle free of gain. In addition to this, we are surprised to see that C_{sca} around the dip frequency decreases significantly as a result of the optical gain and reaches its minimal value of 3.98×10^{-4} nm^2 for the case of $\lambda = 684$ nm and $\varepsilon'' = 0.248$. This value is smaller by 4 orders in magnitude of the scattering cross-section's dip value of the nanoparticle without gain, which makes the nanoparticle difficult to be detected by external observers. The transition from the ultra-high scattering cross-section to the ultra-low one in the proposed core/shell/shell scatter may find applications in lab on chip type setups.

In figures 4(a) and (b), we show the scattering and absorption cross-section spectra at the critical gain, $\varepsilon'' = 0.265$, which is most interesting for the performance as a spaser. We see that the scattering curve exhibits a peak C_{sca} of 2.88×10^5 nm^2 at the resonant wavelength of $\lambda = 695$ nm.

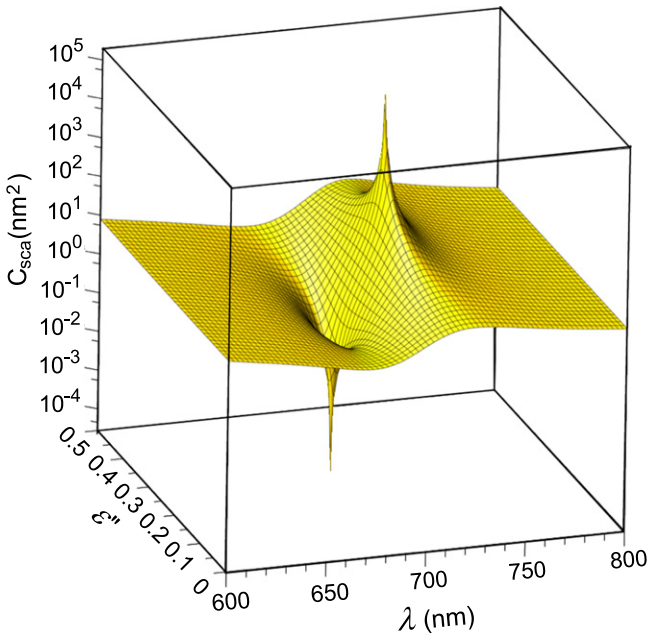

Figure 3. Quasi-static analysis of scattering cross-section of the gain-assisted core/shell/shell nanoparticle as a function of optical gain and wavelength.

Moreover, the linewidth of the scattering spectrum decreases remarkably, resulting in a quality factor as high as 2317. At the same wavelength, the absorption curve shows a dip C_{abs} of -2.56×10^5 nm^2. In our simulation, the critical gain slightly moves to $\varepsilon'' = 0.261$, and the scattering curve shows a peak C_{sca} of 2.39×10^5 nm^2 with the peak wavelength slightly redshifting to 700 nm. Similarly, the absorption curve by simulation shows a dip C_{abs} of -2.40×10^5 nm^2 at 700 nm. At the resonant wavelength, the scattering due to the localized surface plasmon resonance of the nanoparticle is enhanced by more than 4 orders in magnitude and the ohmic loss in metal is almost completely compensated by light amplification from the gain medium. That is, the energy stored through the stimulation of the gain medium can be transferred to the metal to almost completely offset the dissipation of the nanoparticle by means of plasmonic resonance. Our simulation results are in good accordance with the results by quasi-static analysis, except a slight shift of the critical optical gain and resonant wavelength.

To illustrate further the dependency of optical cross-section on the gain layer, we plot in figures 5(a) and (b) the scattering and absorption cross-sections at the resonant wavelength as functions of ε''. When optical gain is increased in the core/shell/shell system, the magnitude of C_{sca} starts to increase smoothly. When ε'' approaches a critical value, C_{sca} first jumps up rapidly to its maximum value then fall down to near zero as ε'' increases over the critical value. This critical gain is similar to the threshold of a classical laser, which we denote as threshold gain, ε''_{thre}. Clearly, in the core/shell/shell system, ε''_{thre} reaches a reasonable value of 0.265 by quasi-static analysis, which is very little different from the simulated value of 0.261. The absorption curve in figure 5(b) shows a different feature. As the increasing of ε'', the absorption is first enhanced smoothly, then climbs to its maximum value when approaching the threshold gain. Different to the scattering feature, the absorption cross-section experiences a rapid transition from positive (maximum) to negative (minimum) at $\varepsilon'' = \varepsilon''_{thre}$. When exceeding the critical gain, C_{abs} quickly move back to near zero.

The dependence of optical cross-section on the gain level is closely related with the localized field distribution of the core/shell/shell nanoparticle. In figure 6, we examine the dependence of the maximum amplitude of the localized electric field of the proposed configuration on the optical gain by numerical simulations. It reveals that the near field amplitude strongly relies on the optical gain. When compared with figure 4(a), it is clearly seen that the near field enhancement follows the evolution trend of scattering cross-section and has a maximum value at $\varepsilon'' = 0.261$. The simulated electric field amplitude distributions (normalized to incident amplitude) of the nanoparticle at resonance (695 nm) are plotted in the insert of figure 6, which shows an electric dipole-like mode with localized electric field as high as 3435 times of the incident field. Such a high localized field enhancement directly results in the amplification of surface plasmon resonance and the scattering cross-section. Although the maximum of the electrical field is located inside the dielectric part, the electrical field outside the nanoparticle is still several hundred times higher than the incident field.

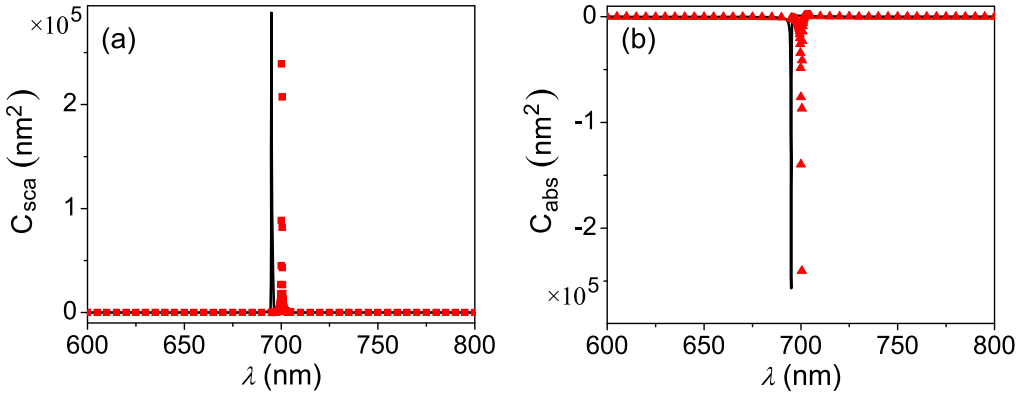

Figure 4. (a) Scattering cross-section and (b) absorption cross-section spectra of a gain-assisted core/shell/shell nanoparticle; solid curves and discrete dots refer to the results by quasi-static analysis (with $\varepsilon'' = 0.265$) and numerical simulations (with $\varepsilon'' = 0.261$), respectively.

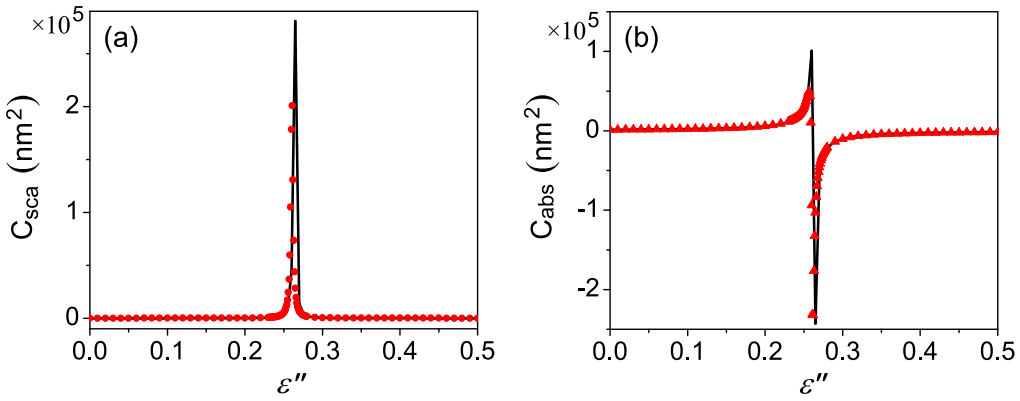

Figure 5. (a) Scattering cross-section and (b) absorption cross-section of core/shell/shell nanoparticle at resonant wavelength as funtions of optical gain; solid curves and discrete dots refer to the results by quasi-static analysis (λ = 695 nm) and numerical simulations (λ = 700 nm), respectively.

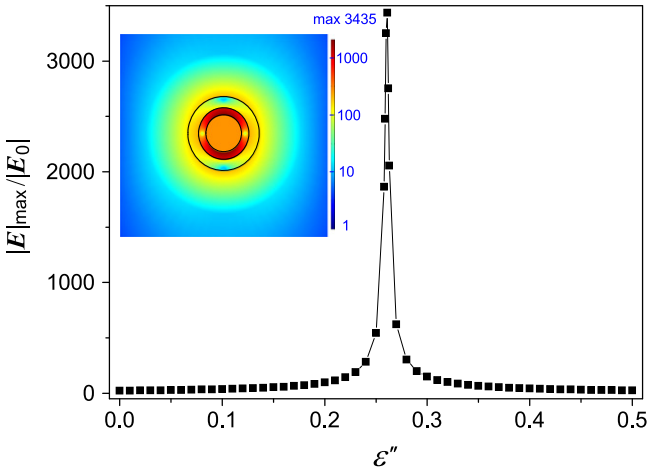

Figure 6. Dependence of near field enhancement $|\vec{E}|_{\max}/E_0$ on optical gain. Insert shows the numerical near field amplitude distribution (normalized to the average incident amplitude) at the resonance when $\varepsilon'' = 0.261$.

Therefore, with no severe impediment, this nanoparticle could be used for applications that require an enhanced field much higher than the incident field.

3. Conclusions

In summary, we have proposed a scheme for controlling the optical cross-section in a gain-assisted metal–dielectric–metal concentric core/shell/shell nanoparticle using quasi-static analysis and finite-element simulations. It was demonstrated that a strongly amplified scattering cross-section accompanied with a negative absorption cross-section can be realized by introducing a suitable amount of gain into the nanoparticle. We revealed that the proposed configuration can behave as an optical switcher whose scattering can be switched from an ultra-high value to an ultra-low one. We further investigated that near field enhancement of the proposed nanoparticle at the plasmonic resonance can be actively controlled by modulating the optical gain in the sandwiched layer. The proposed nanoparticle may find extensive applications in biosensing, optical switching, data storage, as well as on-chip plasmon generation.

Acknowledgments

The work is supported by the Australian Research Council, through its Discovery Grant scheme under grants DP110100713 and DP140100883.

References

[1] Bergman D J and Stockman M I 2003 Surface plasmon amplication by stimulated emission of radiation: quantum generation of coherent surface plasmons in nanosystems *Phys. Rev. Lett.* **90** 027402
[2] Noginov M A, Zhu G, Belgrave A M, Bakker R, Shalaev V M, Narimanov E E, Stout S, Herz E, Suteewong T and Wiesner U 2009 Demonstration of a spaser-based nanolaser *Nature* **460** 1110–2
[3] Oulton R F 2012 Plasmonics: loss and gain *Nat. Photonics* **6** 219–21
[4] Stockman M I 2008 Spasers explained *Nat. Photonics* **2** 327–9
[5] Gordon J A and Ziolkowski R W 2007 The design and simulated performance of a coated nano-particle laser *Opt. Express* **15** 2622–53
[6] Zheludev N I, Prosvirnin S L, Papasimakis N and Fedotov V A 2008 Lasing spaser *Nat. Photonics* **2** 351–4
[7] Li Z and Xia Y 2010 Metal nanoparticles with gain toward dingle-molecule detection by surface-enhanced raman scattering *Nano Lett.* **10** 243–9
[8] Popov O, Zilbershtein A and Davidov D 2006 Random lasing from dye-gold nanoparticles in polymer films: enhanced gain at the surface-plasmon-resonance wavelength *Appl. Phys. Lett.* **89** 191116
[9] Flynn R A, Kim C S, Vurgaftman I, Kim M, Meyer J R, Makinen A J, Bussmann K, Cheng L, Choa F S and Long J P 2011 A room-temperature semiconductor spaser operating near 1.5 μm *Opt. Express* **19** 8954–61
[10] Premaratne M and Agrawal G P 2011 *Light Propagation in Gain Media: Optical Amplifiers* (Cambridge: Cambridge University Press)
[11] Stockman M I 2011 Nanoplasmonics: past, present and glimpse into future *Opt. Express* **19** 22029–106

[12] Stockman M I 2010 The spaser as a nanoscale quantum generator and ultrafast amplifier *J. Opt.* **12** 024004
[13] Liu S Y, Li J, Zhou F, Gan L and Li Z Y 2011 Efficient surface plasmon amplification from gain-assisted gold nanorods *Opt. Lett.* **36** 1296–8
[14] Lisyansky A A, Nechepurenko I A, Dorofeenko A V, Vinogradov A P and Pukhov A A 2011 Channel spaser: coherent excitation of one-dimensional plasmons from quantum dots located along a linear channel *Phys. Rev.* B **84** 153409
[15] Jensen T R, Malinsky M D, Haynes C L and Duyne R P V 2000 Nanosphere lithography: tunable localized surface plasmon resonance spectra of silver nanoparticles *J. Phys. Chem.* B **104** 10549–56
[16] Anker J N, Hall W P, Lyandres O, Shah N C, Zhao J and Duyne R P V 2008 Biosensing with plasmonic nanosensors *Nat. Mater.* **7** 442–53
[17] Zhang H, Zhou J, Zou W and He M 2012 Surface plasmon amplification characteristics of an active three-layer nanoshell-based spaser *J. Appl. Phys.* **112** 074309
[18] Monticone F, Argyropoulos C and Alu A 2013 Multilayered plasmonic covers for comblike scattering response and optical tagging *Phys. Rev. Lett.* **110** 113901
[19] Wu D, Jiang S and Liu X 2011 Tunable fano resonances in three-layered bimetallic Au and Ag nanoshell *J. Phys. Chem.* C **115** 23797–801
[20] Sikdar D, Rukhlenko I D, Cheng W and Premaratne M 2013 Unveiling ultrasharp scattering-switching signatures of layered goldgold nanospheres *J. Opt. Soc. Am.* B **30** 2066–74
[21] Saxena D, Mokkapati S, Parkinson P, Jiang N, Gao Q, Tan H H and Jagadish C 2013 Optically pumped room-temperature GaAs nanowire lasers *Nat. Photonics* **7** 963–8
[22] Wijesinghe T, Premaratne M and Agrawal G P 2014 Electrically pumped hybrid plasmonic waveguide *Opt. Express* **22** 2681–94
[23] Zeman E J and Schatz G C 1987 An accurate electromagnetic theory study of surface enhancement factors for silver, gold, copper, lithium, sodium, aluminum, gallium, indium, zinc, and cadmium *J. Phys. Chem.* **91** 634–43
[24] Berciaud S, Cognet L, Tamarat P and Lounis B 2005 Observation of intrinsic size effects in the optical response of individual gold nanoparticles *Nano Lett.* **5** 515–8
[25] Maier S 2007 *Plasmonics: Fundamentals and Applications* (Berlin: Springer)